

Estimation of CO₂ Storage Capacity Coefficients in Geologic Formations

A. Kopp^a, P. Probst^a, H. Class^a, and R. Helmig^a

^aDepartment of Hydromechanics and Modelling of Hydrosystems, Universität Stuttgart, Pfaffenwaldring 61, 70569 Stuttgart, Germany

This work investigates the effects of several reservoir parameters like absolute and relative permeability, heterogeneity, depth etc. on CO₂ storage capacity of saline aquifers. A sophisticated methodology to estimate CO₂ storage capacity is illustrated and used. Typical reservoirs are defined by analysing a large parameter database. Detailed storage capacity coefficients are given for these typical reservoirs. In the second part, a complex field case example is investigated. This reservoir shows highly heterogeneous permeability and porosity characteristics.

1. INTRODUCTION

The variety of approaches and methodologies to assess CO₂ storage capacity is large, as outlined by Bachu et al. (2007). As a consequence, the estimates of storage capacity are widely varying and sometimes even conflicting. In an attempt to consider several aspects of CO₂ storage capacity, i.e. various process-dependent time scales, different assessment scales (basin, regional, local, or site scale), different assessment types, and different geological storage options, Bachu et al. (2007) propose using the concept of *Resource-Reserve Pyramids*. Out of several pyramids defined therein, we refer here to the *Techno-Economic Resource-Reserve pyramid*, which reflects the degree of uncertainty together with the economic feasibility associated with a capacity estimate by its place on the pyramid. The ‘effective storage capacity’ reflects therein the part of the total porespace which can practically be used for storage considering geological and engineering constraints. Economic aspects, as well as legal, regulatory and infrastructure aspects are still neglected on this level. The estimation of the effective storage capacity of a reservoir is a task which can nicely be tackled by numerical reservoir simulation. However, its not possible to give a general estimate of storage capacity just by looking at the reservoir size. As outlined above, several geological and engineering reasons do influence storage capacity of a reservoir, i.e. absolute and relative reservoir permeability, permeability heterogeneity, reservoir depth, temperature, salinity, etc. as well as injection well location and screening depth. Two types of investigations are illustrated in the following. In the first part, a reservoir parameter database is analysed for statistical characteristics, which are used then to define typical reservoirs like a median reservoir. For several reservoirs defined, detailed storage capacity coefficients (Doughty et al., 2001) are given. In the second part, the CO₂SINK projects reservoir in Ketzin (Germany) is investigated. This highly

heterogeneous formation is well explored and a geological model has been built reflecting the reservoirs muddy flood-plain-facies rocks alternating with sandy string-facies rocks.

2. DEFINITION OF STORAGE CAPACITY

Effective storage capacity can be estimated by a methodology proposed by Doughty et al. (2001). The authors define an effective storage capacity coefficient C , which reduces total storage formation volume ($V_{\text{total}} = \iiint dx dy dz$) to effective capacity (note that theoretical capacity, i.e. pore volume reduced by residual liquid saturation, is not explicitly included in this methodology). Consequently, the effective capacity coefficient C ranges between zero (no storage is possible) to the average formation porosity reduced by residual liquid saturation (all theoretically accessible pore volume is occupied by CO_2). It can be calculated as product of four factors

$$C = C_i \cdot C_g \cdot C_h \cdot \phi_{\text{avg}}, \quad (1)$$

where C_i is the intrinsic capacity coefficient [-], C_g is the geometric capacity coefficient [-] and C_h is the heterogeneity capacity coefficient [-] and ϕ_{avg} is average formation porosity [-]. The intrinsic capacity coefficient C_i is defined as the sum of the fraction of pore space that is occupied by the CO_2 phase (C_{ig}) and the fraction of the pore space that dissolved CO_2 would occupy if it was converted to the gas phase (C_{il}). The intrinsic capacity coefficient C_{ig} can be estimated as the the average gas saturation of the CO_2 plume. The coefficient C_{il} is estimated by $C_{\text{il}} \cong S_1 \cdot X_1^{\text{g}} \cdot \frac{\rho_l}{\rho_{\text{g}}}$, where S_1 is the average liquid saturation, X_1^{g} the average mass fraction of gas dissolved in the liquid phase [kg/kg], and ρ is mass density [kg/m³]. Parameters and variables S_1 , X_1^{g} , ρ are averaged behind the CO_2 front. The geometric capacity coefficient C_g accounts for the reduction of storage capacity by partially penetrating wells, gravity segregation and dipping aquifers. It is defined here as the volume fraction of the entire pore space, occupied by gas, divided by the entire available pore space of the reservoir. The heterogeneity capacity coefficient C_h accounts for heterogeneities in absolute permeability, leading to a further reduction or increase in accessible storage capacity. Figure 1 (Left to Center-Right) illustrates the storage capacity coefficients defined so far.

For investigations on CO_2 storage capacity coefficients on large time scales the definition given by Doughty et al. (2001) is extended. This is to account for the fact, that after tens to hundreds of years, the pore volume covered by the gas phase is different (considerably smaller) than the pore volume covered by brine with dissolved CO_2 load (see Figure 1 (Right)). Consequently, the geometric capacity coefficient C_g is split into two coefficients, C_{gg} and C_{gl} , and intrinsic capacity coefficients C_{ig} and C_{il} are averaged over the respective pore volume fraction. This is, C_{ig} is averaged over the pore volume occupied by gas (C_{gg}), whereas C_{il} is averaged over the pore volume occupied by brine with dissolved CO_2 load (C_{gl}). Since in a complex heterogeneous reservoir no individual estimation on C_g and C_h can be made, the capacity coefficient C_h is also split into two new coefficients, i.e. C_{hg} and C_{hl} . This leads to the following extended definition of storage capacity coefficient C



Figure 1. Estimation of storage capacity coefficients depending on model complexity (after Doughty et al. (2001)); blue colour indicates water phase, yellow colour gas phase and red colour CO_2 dissolved in brine. Left: Estimation of intrinsic storage capacity coefficient (C_i) in a gravitation free, homogeneous reservoir ($C_g = C_h = 1$). Left-Centre: Estimation of the intrinsic (C_i) and geometric (C_g) storage capacity coefficients in a homogeneous reservoir ($C_h = 1$). Right-Centre: Estimation of the intrinsic (C_i), geometric (C_g), and heterogeneity (C_h) storage capacity coefficients in a heterogeneous reservoir. Note that in the latter case, only the product of C_g and C_h can be estimated, since individual contributions can not be identified. Right: Volumetric share (yellow) and dissolved share (yellow+red) according to Equation 2.

$$C = \underbrace{C_{ig} \cdot (C_{gg} \cdot C_{hg}) \cdot \phi}_{\text{volumetric share}} + \underbrace{C_{il} \cdot (C_{gl} \cdot C_{hl}) \cdot \phi}_{\text{dissolved share}} \quad (2)$$

Note that resulting C , as given by Equations 1 and 2, is equal. Individual capacity coefficients leading to the resulting C however, are differently displayed. Having calculated the effective storage capacity coefficient, the effectively stored CO_2 mass, M_{eff} , can be calculated by multiplication with CO_2 density and total geometric reservoir volume (bulk volume). Total geometric reservoir volume is used here, since average reservoir porosity and irreducible liquid saturation (inherently) are included in the coefficient C .

$$M_{\text{eff}} = C \cdot V_{\text{total}} \cdot \rho_{\text{CO}_2}(T, p). \quad (3)$$

Note that carbon density changes with time, since it is generally dependent on changing pressure and temperature conditions. Moreover, C changes with time due to CO_2 injection, plume migration and state of the CO_2 (free-phase, dissolved, chemically bound, etc.) and thus due to changing storage capacity coefficients. Consequently, M_{eff} is time dependent and always equal to the accumulated CO_2 mass in the storage reservoir.

3. SIMULATION ENVIRONMENTS

The general-purpose numerical simulator MUFTE_UG (Bielinski (2006)) is used for the numerical examples shown in Section 4.1. Several modules of different complexity have been especially designed to simulate CO_2 storage in saline aquifers. Here, the approach of two immiscible fluid phases in a homogeneous porous medium is used for investigations on

flow and transport processes during CO₂ storage in geological formations on a short time scale. In Section 4.2, the numerical simulator ECLIPSE300 with the CO2STORE-Option Schlumberger (2008) is used to simulate flow and transport processes in a heterogeneous medium on the short to medium time scale.

4. NUMERICAL EXPERIMENTS

4.1. Radially Symmetric Homogeneous Reservoirs

For investigations on CO₂ storage capacity coefficients and effective mass stored, a 3-D radially symmetric domain is defined. The domain has a radius of 4000 m and a constant height of 100 m. Injection occurs at the centre boundary with a constant rate of 1 MtCO₂ per year. This resembles the annual CO₂ production of a medium-sized coal-fired power plant. Top and bottom boundaries are closed for water and CO₂. At the lateral boundary, fully water saturated conditions and hydrostatic pressure are assumed. The reservoir volume is limited by assuming a ‘virtual’ spill point in 1 kilometre distance from the injection well, i.e. calculations of the geometric capacity coefficient C_g are based on a total geometric reservoir volume of 0.314 km³. Since ϕ is 0.2 in all cases, the available pore space for storage is 0.063 km³. Once CO₂ reaches the virtual spill point, the simulation is stopped.

4.1.1. STATISTICAL CHARACTERISTICS OF RESERVOIR PARAMETERS

Statistical characteristics of reservoir parameters relevant for storage capacity can be calculated from the U.S. National Petroleum Council public database (NPC, 1984). Detailed results and further information on the analysis of the NPC database is given in Kopp et al. (2009) (Part 1). Using the statistical characteristics of the reservoir parameters calculated from the NPC database allows to define typical reservoirs. For the Median reservoir case (further referred to as ‘Case M’), median reservoir parameters for absolute permeability (123 mD), geothermal gradient (0.03 °/m), porosity (20 %) and depth below surface (1524 m) are used. Salinity is also derived from the NPC database, but statistics are not used any further. Instead the median value is used, i.e. 0.048 kg/kg. Same median parameters are used together with the 5th and 95th percentile values for the geothermal gradient (0.018 °C/m and 0.062 °C/m respectively), to define the Cold and Warm reservoir cases (Cases C and W). Similarly, median parameters are used together with the 5th and 95th percentile values for the reservoir depth (386 m and 3495 m respectively) to define the Shallow and Deep reservoir cases (Cases S and D). Note that the Shallow case reservoir depth leads to CO₂ sub-critical conditions). Additional setups include median reservoir properties in addition to measured relative permeability data from formations in the Alberta basin in Canada (Bennion and Bachu, 2008) (Cases V (Viking formation), E (Ellerslie formation), and B (Basal formation)), a setup with tripled entry pressure for the Brooks and Corey capillary pressure model (Case P), a case with a by one order of magnitude reduced absolute permeability (Case K) and a case where CO₂ is injected at half rate. The system is considered to be hydrostatic and in thermal equilibrium, which allows to calculate pressure and temperature conditions at the depth of interest along with delineation of fluid properties.

4.1.2. Results

Figure 2 shows the variation of the capacity coefficients versus effective mass stored M_{eff} . At the end-points of the lines, the CO_2 plume reaches the virtual spill point of the reservoir. The Median case reservoir setup (M), for example, shows medium gravity segregation, compared to the others, which results in a maximum C_g of 0.279 and C_{ig} ($\cong S_g$) of 0.3325, which results in C equal to 0.0188 after 3.85 years of continuous injection, i.e. 3.85 MtCO_2 are stored (M_{eff}). Note, that ρ_{CO_2} equals 660.7 kg/m^3 in Case M.

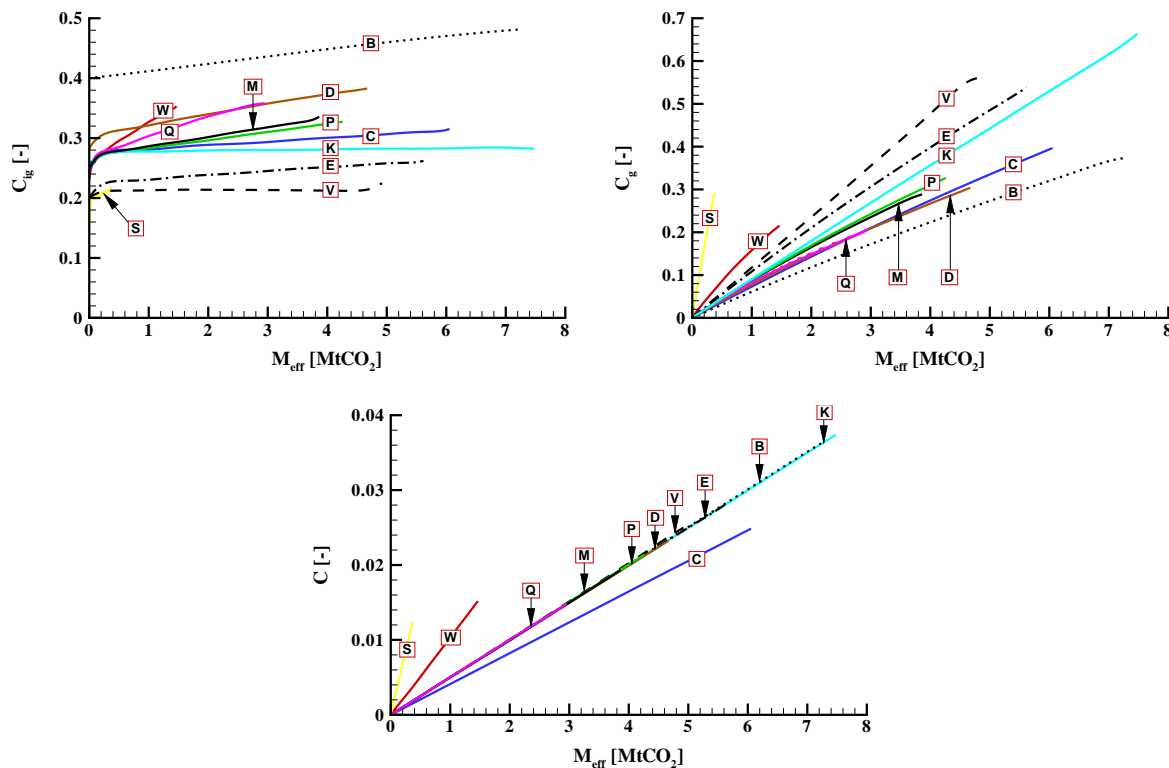


Figure 2. Intrinsic gas-phase capacity coefficient C_{ig} ($\cong S_g$) (left), geometric capacity coefficient C_g (middle) and effective storage capacity coefficient versus effective mass stored M_{eff} . Since in all cases 1 MtCO_2 per year is injected, M_{eff} is equal to time in years (except for case Q, here time is equal to doubled M_{eff}).

Depending on the reservoir parameter setup, the cases show different variation of capacity coefficients and thus a different effective mass stored over time. For example, the Shallow and Warm reservoir setups show, due to low CO_2 density, strong gravity segregation and consequently a lower C and M_{eff} than the Median case (virtual spill point is reached earlier). Cold reservoir setups and those with reduced permeability show a more cylindrical plume evolution, i.e. a larger geometric capacity coefficient, which is due to higher viscosity or lower permeability. The average CO_2 saturation is comparable and thus C and M_{eff} are larger, compared to the Median case. The Median case setups with

relative permeability relations from the Viking and Ellerslie formation show a faster plume evolution than the Median case. This is because of the generally lower CO_2 saturation in the reservoir (and thus lower C_{ig}). However, the much larger C_{g} outweighs the lower C_{ig} , leading to larger effective storage coefficient C and larger M_{eff} . In comparison, the Median case with the relative permeability relation from the Basal formation and the deep reservoir setup show a much slower plume evolution velocity (due to higher C_{ig}) and additionally a higher geometric capacity coefficient C_{g} leading also to a larger effective storage coefficient C and larger M_{eff} . The tripled entry pressure leads to an increase in the geometric capacity coefficient C_{g} along with a similar C_{g} compared to the Median case and thus a larger C and larger M_{eff} . In the case of halvened injection rate (Q) the geometric capacity coefficient is much smaller, consequently C and M_{eff} are lower. In other words this indicates that a high injection rate is advantageous. Since all effective capacity coefficients C with comparable density (all cases except S, W, and C) lie on one line, one can easily see the ordering of cases with respect to C and consequently effective mass stored, i.e. Case Q is worst whereas Case K is most advantageous. Kopp et al. (2009) (Part 1 and 2) provide a more detailed discussion on resulting storage capacity coefficients, depending on reservoir parameter effects and case setups. The author also points out how storage capacity is influenced by buoyancy, viscous and capillary forces by dimensional analysis.

4.2. Heterogeneous Dome-Shaped Reservoir

Carbon dioxide storage capacity coefficients are estimated in a field case example, the Ketzin reservoir of the CO2SINK project (<http://www.co2sink.org>). The Stuttgart formation of the Ketzin reservoir comprises muddy flood-plain-facies rocks alternating with sandy string-facies rocks of good reservoir properties that may attain a thickness of several tens of meters, where sub-channels are stacked. Extensive surveys (seismic profiles, stratigraphic and lithological information) and the three boreholes (one injection well and two observation wells) confirm these assumptions and the information from all measurements provide a basis for the facies and petrophysical modelling. Figure 3 gives an impression of the reservoir and shows the location of the injection and observation wells.

The reservoir is located at a depth of about 600 m below ground surface, which might lead to a change of state of the injected CO_2 , i.e. liquid/supercritical CO_2 changes to gaseous state. For the investigations a continuous CO_2 injection at a rate of 86.4 tons/day over a timespan of nearly 2 years is assumed, i.e. a total mass of 60000 tons of pure CO_2 is injected into the Ketzin reservoir. The fracture pressure of the overlying caprock is never exceeded in the simulations. For a detailed description of the simulation model see Probst (2008). The author gives detailed results on effective storage capacity coefficients based on extensive sensitivity analyses investigating different Net-to-Gross ratios, injection regimes, brine salinity and relative permeability relations, along with a thorough grid convergence study focusing on CO_2 gravity override. To investigate storage capacity coefficients, reservoir size needs to be defined in some way to delineate potential pore volume available for storage purposes. In numerical modelling, it is obvious to choose model domain size. This is, however, not always a good choice, since model domains are often chosen too small to save computational costs, or they are chosen too large to limit influence of the outer boundary conditions on results (to mimic an infinite aquifer). For

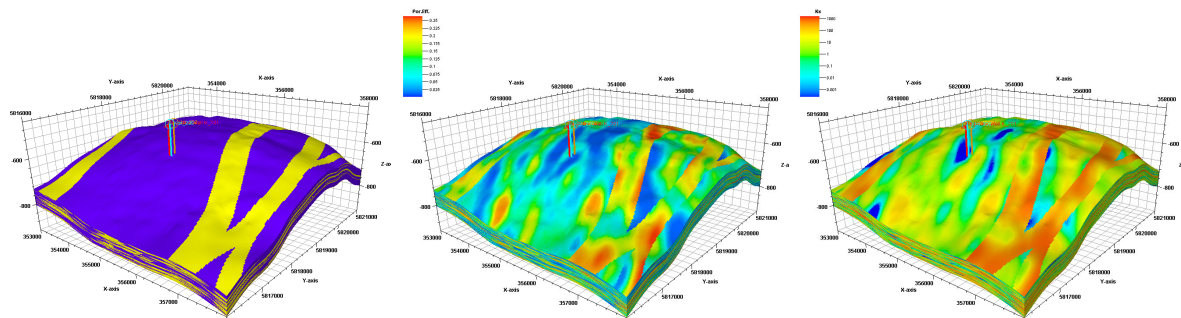


Figure 3. Facies model showing flood-plain-facies rocks alternating with sandy string-facies rocks, effective porosity [-] and intrinsic permeability [mD] model for the Ketzin reservoir base case. Location of the injection and observation wells is indicated at the flank of the dome.

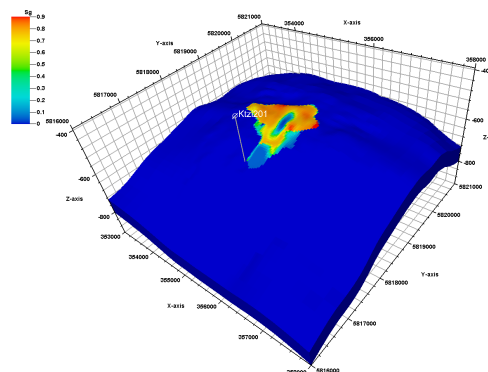


Figure 4. Carbon dioxide saturation after 100 years modelling time.

the Ketzin aquifer, we have chosen a more *realistic* reservoir size by considering the volume between the caprock and above the lowest slotted liner performance in the injection well, i.e. a cap in the top of the domed structure, as the storage reservoir. This *cap* has a volume of $92.8 \cdot 10^6 \text{ m}^3$. Only one per mill of the total injected CO_2 mass leaves this cap after one hundred years, which can be addressed to numerical diffusion of dissolved CO_2 . This indicates that this cap is the reservoir volume utilised for storage.

4.2.1. Results

In Figure 4 the CO_2 saturation is shown after 100 years model time. Carbon dioxide accumulates below the caprock at the top of the dome-shaped formation.

In Figure 5 (left) the partitioning of the injected CO_2 mass in mobile CO_2 (gas phase), dissolved CO_2 in brine and trapped CO_2 (gas phase below residual gas saturation) versus time is shown. It is further distinguished between CO_2 located in the floodplain-facies rocks and in the sandy string-facies rocks (channels). More than 75% of the injected CO_2 are mobile at injection shut-in (after 2 years); of this mobile CO_2 more than 80%

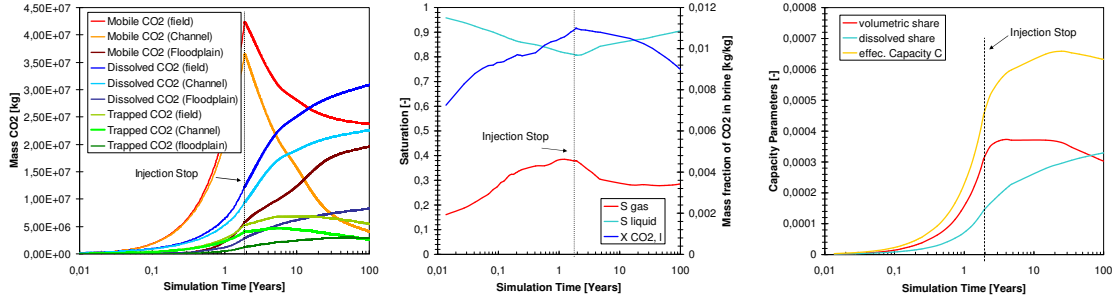


Figure 5. Left: Mobile, residual and dissolved mass for the field and their partitioning between the facies sand-channel and floodplain. Centre: Variation of average mass fraction of CO_2 in brine, average gas and water saturation. Note that the saturations do not add up to one, since they are averaged over different areas (c.f. Section 2). Right: Volumetric share, dissolved share and effective capacity C ; after shut-in, the volumetric share does not increase any more, whereas the dissolution process still goes on.

are located in the channel facies. The mobile CO_2 fraction decreases then with time due to dissolution. After 12 years more CO_2 mass is dissolved in brine than mobile. This can be addressed to the computational grid. Carbon dioxide mass dissolved in brine is overestimated here. A smaller grid size would reduce CO_2 mass dissolved in brine. However, due to already high computational cost, a finer grid cannot be realized. After 100 years only a small amount of mobile CO_2 mass is left within the channel facies, whereas the amount of mobile CO_2 in the floodplain is still increasing. Interesting to notice, that the mass of trapped CO_2 is decreasing again. This can be addressed to the reimbibition process of freshwater into gas filled pore volume and dissolution of trapped CO_2 .

When looking at the average saturation in Figure 5 (centre), a continuous increase of CO_2 saturation within the gas flooded pore volume is apparent up to injection shut-in. Simultaneously, the average liquid saturation is decreasing. After shut-in the reverse effect occurs due to dissolution of gaseous CO_2 . The average mass fraction of CO_2 dissolved in brine increases also up to injection shut-in and decreases then. This occurs despite a continuous dissolution process and increase of dissolved CO_2 mass due to an increase in the pore volume where brine with CO_2 load is found (which serves as the basis for volume averaging).

Summarising, variation of the effective storage capacity coefficient with time is given in Figure 5 along with the associated volume and dissolved share (c.f. Equation 2). The dissolved share is ever increasing with time. The volumetric share increases until shortly after injection stop, and decreases then until stop of simulation. The sum of both, the effective capacity C increases up to 20 years, i.e. up to 18 years after injection stop, and decreases then. Note that M_{eff} (c.f. Equation 3) is constantly 60 000 tons after injection shut-in. The variation of C with time after injection shut-in can be addressed to density effects. Up to 18 years after injection stop, CO_2 density decreases due to upward plume migration of free-phase CO_2 . At times later than 18 years after injection stop,

C decreases again, which means CO_2 density increases. This is due to CO_2 dissolved in brine is moving downwards to deeper regions of the reservoir.

5. CONCLUSIONS

This work focused on the estimation of storage capacity coefficients in saline aquifers. We may summarise in the following:

- In the radially symmetric reservoir employing statistical reservoir parameter characteristics, which assumes that the reservoir storage volume is limited by a leaky well in one kilometre distance, and considering a injection rate of 1 Mt CO_2 per year, in all cases the effective storage capacity coefficient C is less than 0.036 in terms of bulk volume and less than 0.18 in terms of pore volume. Effective storage capacity coefficient C ranges between 0.0117 (Case S) and 0.036 (Case K). The same cases also mark the smallest and largest value of effectively stored mass (M_{eff}). This implicates that the shallow reservoir can store less than 5% of the CO_2 that can be stored in an equally-sized reservoir with a 10 times lower permeability at median depth.
- For the highly heterogeneous Ketzin reservoir, considering the definition of the reservoir volume potentially available for CO_2 storage and the injection regime of only 60.000 tons of CO_2 injected within almost two years, the estimated storage capacity coefficient C is 0.6 per mill in terms of bulk volume and 5.7 per mill in terms of pore volume. The location of the injected CO_2 could be shown over time, i.e. CO_2 mass located in the floodplain-facies rocks and in the sandy string-facies rocks. Furthermore, the partitioning of the injected CO_2 mass in mobile CO_2 (gas phase), dissolved CO_2 in brine and trapped CO_2 (gas phase below residual gas saturation) fractions versus time is shown.
- The relative permeability–saturation relationships have proven to be of great influence for storage capacity, they influence the storage capacity estimates to a similar extent as the entire range of reservoir properties like geothermal gradient and depth. The effect relative permeability hysteresis, neglected in this study, will further influence CO_2 storage capacity.
- The authors could show by two examples, that estimation of CO_2 storage capacity coefficients is subject to multiple definitions and assumptions and requires careful interpretation. This is shown when comparing the storage capacity coefficients for the radially symmetric reservoir and the heterogeneous Ketzin reservoir. One observes a difference of one order of magnitude in effective storage capacity coefficient C . This difference is due to the definition of the reservoir volume potentially available for CO_2 storage (fill of a flat reservoir upon arrival of the plume at a virtual spill point versus injection into a dome-shaped reservoir with no arrival at any leakage point) and due to the difference in total injected mass (1 Mt CO_2 per year versus 60000 tons within two years). Carbon dioxide effective storage capacity coefficient C as defined here, is largely influenced by these two constraints.

Acknowledgements

The authors gratefully acknowledge funding by the CO2SINK project (SES6-CT-2004-5025599) sponsored by the Commission of the European Communities and the industry (Statoil, RWE, Vattenfall, and VNG) and by the GEOTECHNOLOGIEN program.

References

- Bachu, S. and Bonijoly, D. and Bradshaw, J. and Burruss, R. and Holloway, S. and Christensen, N.P. and Mathiassen, O.M., CO₂ storage capacity estimation: methodology and gaps, *International Journal of Greenhouse Gas Control*, 1(4), 430–443, 2007.
- Bennion, B. and Bachu, S., Drainage and imbibition relative permeability relationships for supercritical CO₂/brine and H₂S/brine systems in intergranular sandstone, carbonate, shale, and anhydrite rocks, *SPE Reservoir Evaluation & Engineering*, 11(3), 487–496, DOI: 10.2118/99326-PA, 2008.
- Bielinski, A., Numerical Simulation of CO₂ Sequestration in Geological Formations, Universität Stuttgart, Mitteilungsheft Nr. 155, Institut für Wasserbau, Universität Stuttgart, 2006.
- Doughty, C. and Pruess, K. and Benson, S. and Hovorka, S. and Knox, P. and Green, C., Capacity investigation of brine-bearing sands of the Frio-Formation for geological sequestration of CO₂, *Proceedings of First National Conference on Carbon Sequestration*, U.S. Department of Energy, National Energy Technology Laboratory, 2001.
- Kopp, A. and Class, H. and Helmig, R., Investigations on CO₂ Storage Capacity in Saline Aquifers - Part 1: Dimensional Analysis of Flow Processes and Reservoir Characteristics, *International Journal of Greenhouse Gas Control*, in press, 2009.
- Kopp, A. and Class, H. and Helmig, R., Investigations on CO₂ Storage Capacity in Saline Aquifers - Part 2: Estimation of Storage Capacity Coefficients, *International Journal of Greenhouse Gas Control*, in press, 2009.
- NPC, U.S. National Petroleum Council Public Database, <http://www.netl.doe.gov>, 1984.
- Probst, P., Numerical Simulations of CO₂ Injection into Saline Aquifers: Estimation of Storage Capacity and Arrival Times using Multiple Realizations of Heterogeneous Permeability Fields, Diploma Thesis, Institut für Wasserbau, Universität Stuttgart, 2008.
- Schlumberger, Eclipse Technical Manual, 1, 2008.